New Journal of Physics
The open-access journal for physics

Attosecond keV x-ray pulses driven by Thomson scattering in a tight focus regime

D Kim[1], H Lee[1], S Chung[1] and K Lee[2]

[1] Department of Physics, POSTECH, San 31 Hyojadong, Nam Ku, Pohang, Kyungbuk 790-784, Korea

[2] Laboratory for Quantum Optics, Korea Atomic Energy Research Institute, P O Box 105, Yuseong, Daejeon 305-600, Korea

E-mail: kimd@postech.ac.kr

New Journal of Physics **11** (2009) 063050 (12pp)
Received 1 April 2009
Published 30 June 2009
Online at http://www.njp.org/
doi:10.1088/1367-2630/11/6/063050

Abstract. The radiation of a relativistic electron interacting with a co-propagating tightly focused high-power laser is investigated. High-order fields (HOFs) existing in a tight focus (a few micrometers or so) affect the dynamics of electrons rather significantly so as to enhance radiation intensity by several orders of magnitude. In the case of a co-propagating interaction geometry, the second-order field plays an important role in radiation enhancement. It is demonstrated that when HOFs are included, the radiation efficiency is increased by a factor of up to 100 000 for $w_0 = 2$ and 5 μm, with a laser intensity of 2.2×10^{20} W cm^{-2}, compared with that when HOFs are not included. The enhancement is larger for smaller electron energies and laser beam waists.

It has also been shown that when an electron bunch interacts with a high-intensity tightly-focused femtosecond laser pulse in a co-propagation geometry, attosecond (~300 as) x-ray pulses can be produced. The photon energy can reach about 40 keV for an electron energy of 2 GeV. The physical scheme investigated in this work can be used for an ultrafast (attosecond or femtosecond) x-ray source in the range of 10–100 keV.

Contents

1. Introduction

At the beginning of this century, the femtosecond (fs) barrier was broken [1], a door being opened to new opportunities for the study of ultrafast electron dynamics in atoms, molecules and nano-structured systems that have never been explored before. Attosecond technology has been rapidly progressing in which an isolated sub-100 as pulse was demonstrated [2]. The real time observation of inner-shell processes in atoms [3], tunneling ionization from atoms [4], and bandgap transition of electrons in solid has been observed [5]. The currently available photon energy of attosecond pulses is in the soft x-ray region, 30–100 eV. Figure 1 shows ultrafast sources available currently or in the immediate future. It is conspicuous that there is no source available in keV or higher energies faster than 10 fs. In fact, for wider exploration and manipulation of electron dynamics in a vast spectrum of natural phenomena, attosecond or a few fs keV pulses are demanded. In this vein, the present paper proposes a new physical scheme to generate attosecond keV x-ray pulses by utilizing the interaction of a tightly focused fs laser with a relativistic electron beam. High-order fields (HOFs) existing in a tight focus (a few micrometers or so) play key roles to not only produce radiation at keV energies but also enhance the radiation by five orders of magnitude. A ∼300 as pulse in the keV range can be produced. This source will find many applications in the study of ultrafast atomic and chemical dynamics.

In the case of interaction of an electron beam with a laser, there are three major interaction geometries: counter-propagation (Compton back-scattering), 90°-scattering and co-propagation (0°-scattering) geometries. The pulse duration, photon flux and photon energy of the radiation in each case are summarized in table 1. Considering a typical specification of currently available electron beams (i.e. ∼10 ps pulse duration and 30 μm diameter) and fs lasers (i.e. 30 fs), it is easy to note that the co-propagation geometry produces the shortest pulse. However, the radiation produced by the co-propagation interaction in a conventional way is not only very weak but also in the vicinity of the laser wavelength.

How can one then increase photon flux in the co-propagation geometry? Here we show that HOFs existing in a tight focus regime can be utilized to enhance the photon flux. The tight focus here means that the focal spot size is in the order of the wavelength of lasers. The current study shows that HOFs make significant contributions so that keV x-ray photons are produced at high photon flux in the interaction of a tightly focused co-propagating laser with an electron bunch. Maxwell equations tell us that in such a tight focus regime, HOFs cannot be neglected any more and a conventional transverse Gaussian field description of a laser is no longer valid [6]. The proper description of the tightly focused laser beam has been derived in powers of $s = 1/kw_0$,

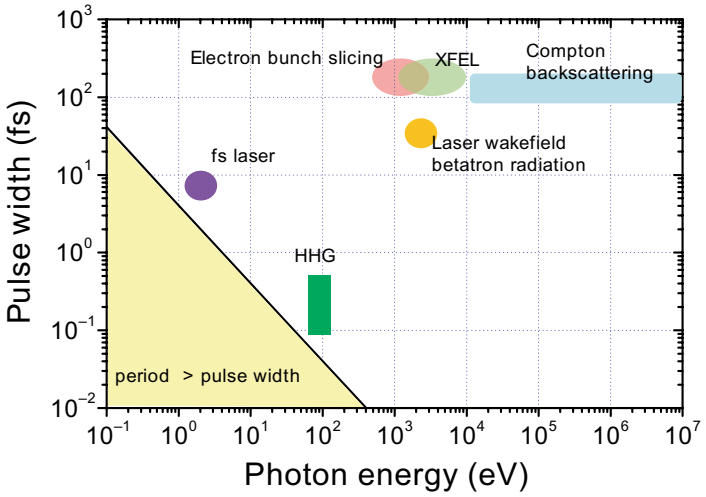

Figure 1. Currently available ultrafast light sources plotted in terms of photon energy and pulse duration. It is obvious that there is no ultrafast (attosecond or less than 10 fs) source in keV and higher energies.

Table 1. Comparison of radiation characteristics between three major interaction geometries. L_{conf}, L_{laser}, L_{el} and L_{T}, are the confocal parameter and the pulse length of a driving laser, the pulse length and diameter of an electron bunch, respectively. c is the speed of light. σ_{T}, n_{e} and n_{L} are the Thomson cross-section and the number of electrons and photons in the interaction, respectively. γ and ω_{L} are the relativistic Lorentz factor and the frequency of the driving laser, respectively. The pulse duration for each interaction geometry in the first column is estimated for a 20 ps, 30 μm diameter electron bunch and a 30 fs, 5 μm diameter focus laser. The co-propagation interaction geometry gives the shortest pulse.

Interaction geometry	Pulse duration of radiation	Photon flux	Photon energy of radiation
Counter-propagation	$\Delta t \sim 2L_{\mathrm{conf}}/c \sim 600$ fs	$2\sigma_{\mathrm{T}} n_{\mathrm{e}} n_{\mathrm{L}}$	$4\gamma^2\omega_{\mathrm{L}}$
90°-scattering	$\Delta t \sim (L_{\mathrm{T}} + L_{\mathrm{laser}})/c \sim 130$ fs	$\sigma_{\mathrm{T}} n_{\mathrm{e}} n_{\mathrm{L}}$	$2\gamma^2\omega_{\mathrm{L}}$
Co-propagation	$\Delta t \sim L_{\mathrm{laser}}/c \sim 30$ fs	$\dfrac{\sigma_{\mathrm{T}} n_{\mathrm{e}} n_{\mathrm{L}}}{2\gamma^2}$	ω_{L}

where $k = 2\pi/\lambda$ and w_0 is the wave number and the beam waist (radius at the best focus), respectively [6]–[9]. Salamin *et al* [10] has obtained HOFs up to the 11th order in a power series of diffraction angle $\varepsilon = 2s$. The HOFs were indeed shown to have significant effects on the laser acceleration of an electron [11]–[13] as well as on the radiation characteristics [14]. The longitudinal component of HOFs was shown to play a significant role in the generation of high-quality electron bunches [15]. In this paper, we demonstrate that the effect of HOFs existing in a tight focus regime on the relativistic nonlinear Thomson scattered (RNTS) radiation by a relativistic electron co-propagating with a laser is dramatic: (i) the radiation intensity per electron can be enhanced 100 000 times and (ii) a few keV photons are produced. No work has been done in this respect.

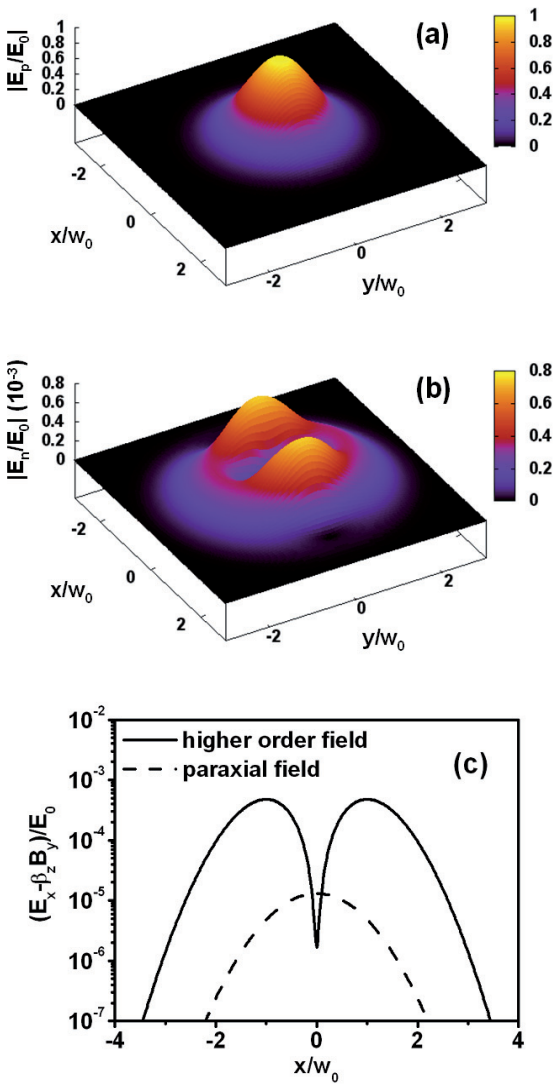

Figure 2. Spatial distribution of the paraxial (the 0th order) field (a) and E_{h} of the HOFs (up to seventh order), (b) on the focal plane at $t = 0$. (c) The x-component of the force sensed by the 100 MeV ($\beta_z \approx 0.999\,98$) electron near the focal plane at $t = 0$ and $y = 0$ (the laser is linearly polarized in the x-direction and propagates in the z-direction).The fields are normalized by the peak electric field strength E_0. The beam waist (w_0) is 5 μm. Note that the force due to HOFs is stronger off-axis.

As shown in figures 2(a) and (b), the spatial profile of the HOF is totally different from that of the 0th order (paraxial) field (Gaussian profile). Even though the HOF amplitude ($\sim 10^{-4}\ E_0$) is much less than the paraxial field amplitude ($\sim 10^{-1}\ E_0$), the HOF can strongly affect electron dynamics. How and when the HOFs have dramatic effect can be understood by examining the Lorentz force exerted on an electron. From the relativistic equation of motion, we can write

$\mathrm{d}\beta_x/\mathrm{d}t\,(\beta_x = v_x/c)$ as follows:

$$\frac{\mathrm{d}\beta_x}{\mathrm{d}t} \approx \frac{e}{m_e c}\gamma^{-1}\left[(1-\beta_z)E_x^{(0)} + \varepsilon^2(E_x^{(2)} - \beta_z B_y^{(2)}) + \cdots\right] \tag{1.1}$$

$$\approx \frac{e}{m_e c}\gamma^{-3}\left[\frac{E_x^{(0)}}{2} + \gamma^2\left\{\varepsilon^2(E_x^{(2)} - B_y^{(2)}) + \cdots\right\}\right], \tag{1.2}$$

where $E_x^{(0)}$, $E_x^{(2)}$ and $B_y^{(2)}$ are the zeroth-order and second-order fields, respectively, and their magnitudes are similar to each other. Since we consider a relativistic electron co-propagating with the laser in the $+z$ direction, $\beta \approx \beta_z \approx 1$ and $1-\beta_z \approx 1/(2\gamma^2)$ are used from equations (1.1) to (1.2), where $\beta = v/c$, $\varepsilon = 2/kw_0$ and $\gamma = 1/\sqrt{1-\beta^2}$, Lorentz factor. The magnitudes of $1/\gamma$ and ε determine which one of the 1st and 2nd terms in equation (1.2) is dominant. We note from equation (1.2) that for $2(\gamma\varepsilon)^2 \gg 1$, the second term is dominant: non-paraxial HOFs become important. This is clearly shown in figure 2(c), which shows the transverse component of Lorentz force near focus exerting on a relativistic 100 MeV electron co-propagating with a laser of 5 μm beam waist. In this case, $2(\gamma\varepsilon)^2 = 200 \gg 1$. Off-axis, the force due to HOFs is indeed larger than that due to the paraxial field. The fact that $2(\gamma\varepsilon)^2 \gg 1$ implies that for a given beam waist, there is a threshold electron energy, beyond which the force due to HOFs becomes dominant. However, as discussed below, due to the spatial profile of HOF, there exists a range of electron energy in which the HOF has a remarkable effect on the characteristics of RNTS.

2. Simulation method

In our simulation, we employed an 800 nm, 5 fs full-width at half maximum (FWHM), linearly polarized (in the x-direction) laser pulse with a peak intensity of 2.2×10^{20} W cm^{-2} ($a_0 = 10$, $a_0 = eE_0/m_e\omega c$ is the normalized vector potential, where E_0 is the laser electric field strength, ω the frequency of the laser, e the electron charge, m_e the electron mass and c the speed of light). In simulations, an electron is initially situated at the peak of the envelope of the laser pulse on the z-axis at $t = -10\,000$ fs. The time $t = 0$ is defined to be the time when the peak of the envelope of the laser pulse passes the position $z = 0$, which is the position of the laser beam waist (the best focus). The electron starts to co-propagate in the $+z$-direction along with the laser pulse and passes through the best focus of the laser field.

2.1. Methods

To evaluate the radiation characteristic from the interaction of laser and electrons, the relativistic equation of motion is numerically solved for the dynamics of an electron [16]. The motion of a single electron in a high-intensity laser field is described by the following relativistic equation of motion:

$$m_e\frac{\mathrm{d}}{\mathrm{d}t'}(\gamma\vec{v}) = -e(\vec{E} + \beta \times \vec{B}),$$

where m_e is the electron mass, $\vec{v}$ the velocity of the electron, γ the relativistic Lorentz factor, $\vec{\beta} = \vec{v}/c$, and $\vec{E}$ and $\vec{B}$ are the electric and magnetic fields of an incident laser, respectively. The fields used in this simulation are those derived by Salamin *et al* [10, 11] in a tight focus regime in terms of the diffraction angle, $\varepsilon = w_0/z_r$, up to the 11th-order, where w_0 is the laser beam waist and z_r the Rayleigh length. The fields E_x, B_y and E_z are written here up to the

second order of ε, for simplicity

$$E_x = E\left\{S_1 + \varepsilon^2\left[\xi^2 S_3 - \frac{\rho^4 S_4}{4}\right] + \cdots\right\},$$
$$B_y = E\left\{S_1 + \varepsilon^2\left[\frac{\rho^2 S_3}{2} - \frac{\rho^4 S_4}{4}\right] + \cdots\right\},$$
$$E_z = E\xi\left\{\varepsilon\left[C_2\right] + \cdots\right\},$$

where $E = E_1 \mathrm{e}^{-r^2/w^2}$, $w = w_0\sqrt{1+(z/z_\mathrm{r})^2}$, $z_\mathrm{r} = \pi w_0^2/\lambda$, $\xi = x/w_0$, $\upsilon = y/w_0$, $\zeta = z/z_\mathrm{r}$ and $\rho^2 = \xi^2 + \upsilon^2$. $E_1 = E_0 \exp\left[-2\ \ln\ 2(t - z/c)^2/\Delta t_\mathrm{L}^2\right]$ where E_0 is the peak electric field and Δt_L is the laser pulse duration. C_n and S_n are defined as

$$C_n = \left(\frac{w_0}{w}\right)^n \cos(\psi + n\psi_\mathrm{G}),$$
$$S_n = \left(\frac{w_0}{w}\right)^n \sin(\psi + n\psi_\mathrm{G}), \quad n = 1, 2, 3, \ldots,$$

where $\psi = \psi_0 + \omega t - kz - kr^2/2R$ and $R = z + z_\mathrm{r}^2/z$. ψ_0 is the constant initial phase and k is the laser wave number, $2\pi/\lambda$. ψ_G is the Guoy phase expressed as $\psi_\mathrm{G} = \tan^{-1}(z/z_\mathrm{r})$.

The angular distribution of the radiated power detected far away from the electron toward the direction $\hat{n}$ at a time t is then calculated as

$$\frac{\mathrm{d}P(t)}{\mathrm{d}\Omega} = |\vec{A}(t)|^2, \qquad \vec{A}(t) = \sqrt{\frac{e^2}{4\pi c}}\left[\frac{\hat{n}\times\left\{(\hat{n}-\vec{\beta})\times\frac{\mathrm{d}\vec{\beta}}{\mathrm{d}t}\right\}}{\left(1-\hat{n}\cdot\vec{\beta}\right)^3}\right]_{t'}$$

where t' is the electron's time or retarded time and related to t by $t = t' + \frac{x - \hat{n}\cdot\vec{r}\,(t')}{c}$.
Then the angular spectral intensity can be obtained by the Fourier transform of $A(t)$ as

$$\frac{\mathrm{d}^2 I}{\mathrm{d}\omega\,\mathrm{d}\Omega} = 2\,|A(\omega)|^2,$$
$$A(\omega) = \frac{1}{\sqrt{2\pi}}\int_{-\infty}^{\infty} A(t)\mathrm{e}^{-\mathrm{i}\omega t}\,\mathrm{d}t.$$

3. Results and discussion

The angular peak powers (the strongest radiation power over a whole range of interaction time and angle of detection) [16] were acquired for various electron initial energies from 10 to 200 MeV and focal spot sizes (or beam waists) of the laser. Figure 3(a) shows the variation of the angular peak power with respect to the initial electron energy for the laser field including the HOFs (solid line) and not including the HOFs (dashed line). The laser beam waist is 5 μm at focus. It is obvious that when the HOFs are included, the radiation is enhanced by several orders of magnitude in a particular energy region (from 20 to 100 MeV) compared with that when the HOFs are not included. Figure 3(b) reveals that higher energy photons (up to a few keV) are also produced due to nonlinear interaction. The inset in figure 3(b) is the spectrum without HOFs.

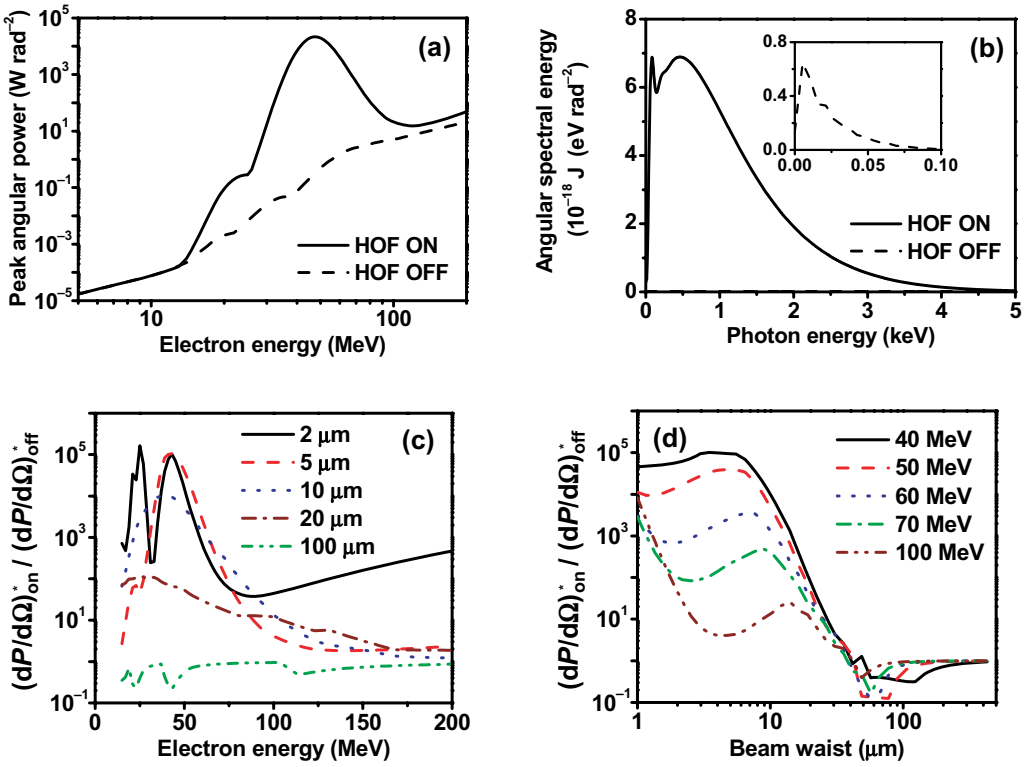

Figure 3. (a) Angular peak power versus initial electron energy when the HOFs (up to the seventh order) are included (solid line) and when the HOFs are not included (dashed line). (b) Spectrum at the peak of radiation power (electron energy: 50 MeV). The inset shows the spectrum when HOFs are not included. (c) Enhancement of the peak power due to HOFs versus electron energy for different beam waists. (d) Enhancement of the peak power with respect to laser beam waist for various electron energies.

The calculation has also been done for different beam waists, keeping the laser intensity constant. The enhancements of radiation power, the ratios of radiation power with HOFs to that without HOFs, are shown in figure 3(c) and (d) for different electron beam energies and laser beam waists. The enhancement can be as large as 100 000 times. The smaller the initial electron energy or the laser beam waist, the larger the enhancement. Even at a laser beam waist of 20 μm, the enhancement is already of the order of 10 (figure 3(d)). This clearly demonstrates that the consideration of HOFs is very important in a tight focus regime.

The enhancement of radiation power can be understood by closely examining the electron dynamics and what factors contribute to the radiation. According to electrodynamics [17], the radiation is strongly emitted when an electron goes through severe acceleration. The simulation reveals that the transverse component of acceleration, $\mathrm{d}\beta_x/\mathrm{d}t$, greatly contributes to the total radiation. The peak of angular radiation power can then be approximated as

$$\left.\frac{\mathrm{d}P(t)}{\mathrm{d}\Omega}\right|_{\mathrm{peak}} \approx \frac{e^2}{4\pi c}\left\{\frac{|\mathrm{d}\beta_x/\mathrm{d}t|^2}{(1-\beta)^4}\right\}_{\mathrm{ret}} \propto \left\{\gamma^8\left|\frac{\mathrm{d}\beta_x}{\mathrm{d}t}\right|^2\right\}_{\mathrm{ret}}. \tag{2}$$

Equation (2) tells us that the angular radiation power is a strong function of transverse acceleration $|\mathrm{d}\beta_x/\mathrm{d}t|$ and the Lorentz factor, γ. $|\mathrm{d}\beta_x/\mathrm{d}t|^*$ and γ^* are plotted in figures 4(a) and (b) for the case of a laser beam waist of 5 μm, respectively. The star (*) means that its value is taken at the time when the electron emits its peak radiation. It is clearly seen that when the initial energy of the electron is in the range of 20–100 MeV, the electron experiences severe acceleration and thereby goes through a large energy gain. The increases in both $|\mathrm{d}\beta_x/\mathrm{d}t|^*$ and γ^* work together to enhance the radiation by a factor of 100 000 at an initial energy of 50 MeV. In figure 4(a), note that $|\mathrm{d}\beta_x/\mathrm{d}t|$, in general, decreases with an increase in the initial electron energy. It scales as γ^{-3} (dashed or dashed-dot line) except in the energy range of 20–100 MeV. Figure 4(b) shows that outside this energy range, γ^* is almost the same as γ_0 (initial γ). For an electron of 10 MeV ($\gamma \approx 20$) or smaller, the 1st term ($\sim 10^{-2}\, E_0$) in the square bracket of equation (1.2) is larger than the second term ($\sim 10^{-6}\, E_0$) so that the first term mainly contributes to $\mathrm{d}\beta_x/\mathrm{d}t$, leading to $\mathrm{d}\beta_x/\mathrm{d}t \propto \gamma^{-3}$. The severe acceleration in the region of 20–100 MeV is closely related to the spatial profile near the focus $z = 0$ of the force field, $E_x - \beta_z B_y$ (or $E_x - B_y$ with $\beta_z \approx 1$) acting on the electron, as shown in figure 4(c). Trajectories of electrons with different initial energies of 30, 50 and 100 MeV are also drawn. As illustrated in figure 4(c) or 2(c), $E_x - \beta_z B_y$ vanishes on-axis, reaches its maximum around $x/w_0 = 1$ and then decreases again. Note that the electron of 30 MeV or smaller is bent too much to pass through the focus (dashed-dot line), the electron of 50 MeV passes through the strong force region (dashed line), and the electron of 100 MeV or higher stays closely on-axis (thin line) where the force is weaker. This explains that electrons with an initial energy in the range of 20–100 MeV experience stronger acceleration than those outside this energy window. This is manifested as a hump in both the $|\mathrm{d}\beta_x/\mathrm{d}t|^*$ and the γ^* plot. Because of the laser intensity and beam waist chosen in this study, a large increase in $|\mathrm{d}\beta_x/\mathrm{d}t|^*$ and γ^* occurs in the energy range of 20–100 MeV. This energy window can move to the higher energy side for larger laser intensity because a higher laser field can bend the trajectory of a higher energy electron.

For electron energies slightly higher than 100 MeV, $|\mathrm{d}\beta_x/\mathrm{d}t|^*$ again becomes proportional to γ^{-3}. Since γ is very large, the electron is less bent and stays closely on-axis where HOF is weak, as shown in figures 4(c) or 2(c), so that the second term of equation (1.2) becomes more or less constant. This results in $\mathrm{d}\beta_x/\mathrm{d}t \propto \gamma^{-3}$ again. The difference in the fitting constants c_1 and c_2 comes from the fact that the electron with a smaller energy is largely bent by the laser field and radiates outside the Rayleigh range where the laser intensity is weak; on the other hand, the electron with a higher energy passes through the focus, experiencing an effectively higher laser field: hence, c_2 is larger than c_1.

Up to now, we have shown that HOFs remarkably affect the radiation characteristics of a single electron interacting with a co-propagating laser in a tight focus regime: (i) keV photons can be produced and (ii) radiation power can be enhanced as much as 100 000 times. For a real source, one has to work with an electron bunch. A series of simulations has been carried out. The laser employed in the simulation has the following specifications: a pulse duration of 5 fs FWHM and a wavelength of 800 nm (or a photon energy of 1.55 eV). The laser was focused down to the 5 μm diameter spot at $z = 0$, where its intensity reaches 2.2×10^{20} W cm^{-2} (normalized vector potential is $a_0 = eE_0/(m\omega c) = 10$). An electron bunch with a charge of 1 nC, an emittance of 2 mm mrad and a diameter of 30 μm is used in the simulation. An electron bunch with these parameters is readily available in the current technology. Since the spatial extent of the 5 fs FWHM pulse is about 3 μm, the length of the electron is limited to 14 μm to minimize computational load. Figures 5(a) and (b) show the temporal structure and the

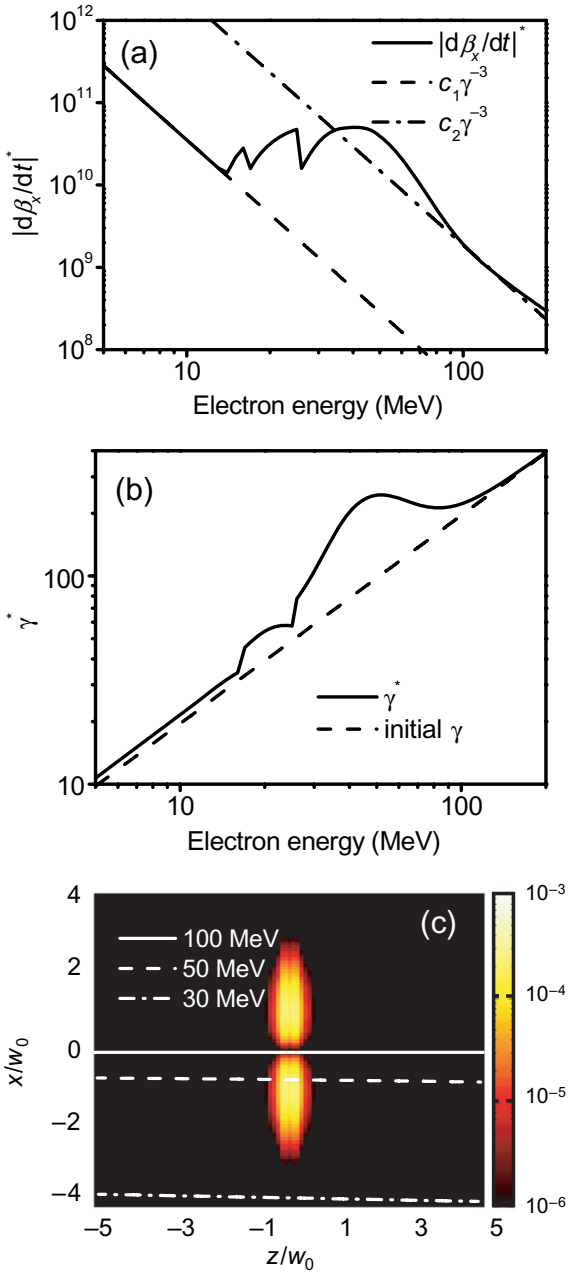

Figure 4. (a) $|d\beta_x/dt|^*$ versus initial electron energy, where the star (*) indicates that it is the value when the electron radiates its angular peak power. (b) The Lorentz factor (solid line) at the time of maximum radiation with respect to initial electron energy. The dashed line represents the initial Lorentz factor. (c) Force field E_x–B_y on the zx-plane at $t = 0$. The color scale represents the magnitude of the force field: white is the strongest force field and black represents no force. The solid, dashed and dashed-dot lines represent electron trajectories for 100, 50 and 30 MeV, respectively. In (a), (b) and (c), the laser parameters are 5 fs, 800 nm, 2.2×10^{20} W cm^{-2} and $w_0 = 5\,\mu$m.

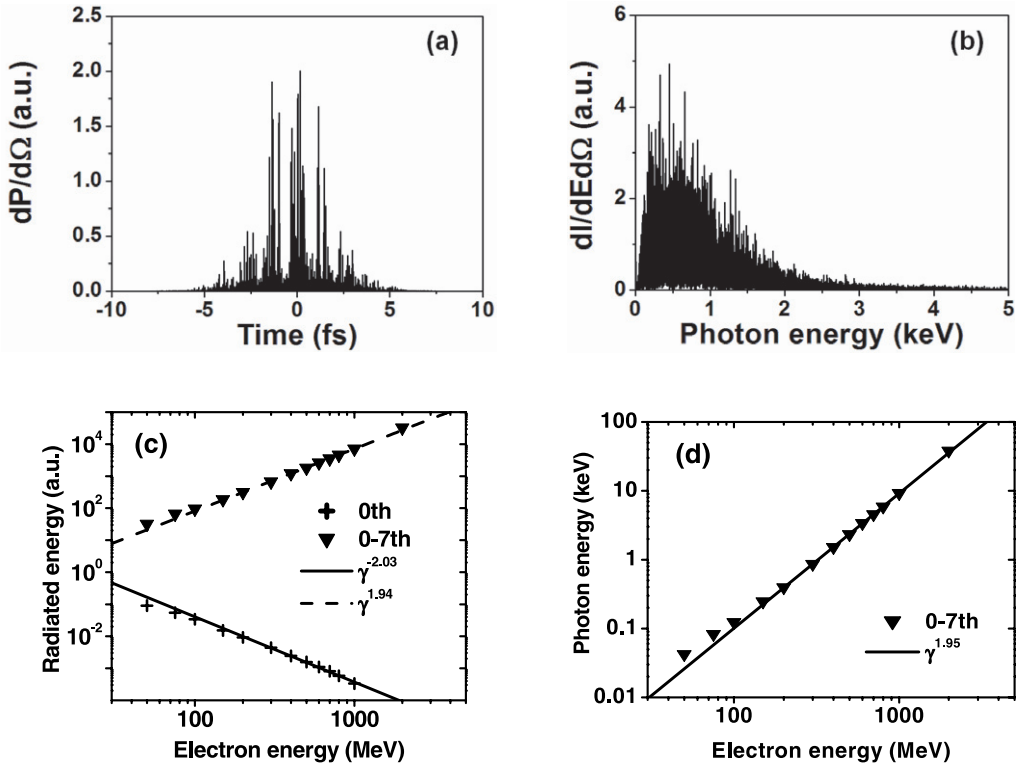

Figure 5. Temporal structure (a) and spectrum (b) of the radiation from the interaction of an electron bunch with a co-propagating tightly focused fs laser. The energy of the electron bunch is 200 MeV and the energy spread is 0.1%. Note that a train of attosecond pulses is generated and keV photons are produced. (c) Dependence of total radiated energy without and with HOFs on initial electron energy. Without HOFs, radiated energy decreases with initial electron energy as $\gamma^{-2.03}$ (cross and solid line); on the other hand, with HOFs, it increases as γ^{+194} (inverse triangle and dashed line). (d) Average photon energy versus γ. The average photon energy scales as $\gamma^{+1.96}$. 40 keV attosecond x-rays can be produced for a 2 GeV electron bunch.

spectrum of the radiation from the interaction of such an electron bunch with a co-propagating tightly focused fs laser. The energy of the electron bunch is 200 MeV and the energy spread is 0.1%. The electron bunch consists of 3.0×10^4 electrons, which are randomly distributed throughout the bunch. The centers both of the electron bunch and the laser meet at the best focus ($z = 0$). The radiation is detected on the z-axis. Figure 5(a) shows that a train of attosecond pulses is generated. The spectrum (figure 5(b)) shows that keV photons are produced.

Figure 5(c) shows the dependence of the total radiated energy without and with HOFs on the initial electron energy. Note the drastic difference between them. Without HOFs, the radiated energy decreases with the initial electron energy as $\gamma^{-2.03}$ (cross and solid lines); on the other hand, with HOFs, it increases as $\gamma^{+1.94}$ (inverse triangle and dashed line). The average photon energy also scales as $\gamma^{+1.95}$, as shown in figure 5(d). Using a 2 GeV electron beam, even 40 keV attosecond x-rays can be produced. The photon number per electron bunch and laser pulse is

calculated to be 4.2×10^6 when an 800 nm, 5 fs FWHM laser pulse with 420 mJ is focused to a beam waist of 5 μm, and interacts with an electron bunch of 100 fs and 1 nC. The large enhancement of the radiation power together with an ultra-short interaction time may lead to the development of new strong ultra-short (attosecond, femtosecond) x-ray sources.

4. Conclusion

The radiation of a relativistic electron interacting with a co-propagating tightly-focused high-power laser is investigated. When a laser is focused tightly, the HOFs cannot be neglected: they affect the dynamics of electrons rather significantly so as to enhance radiation intensity by several orders of magnitude. In the case of a co-propagating interaction geometry, the second-order field plays an important role in the radiation enhancement. It is demonstrated that when HOFs are included, the radiation efficiency is increased by a factor of up to 100 000 for $w_0 = 2$ and 5 μm, with a laser intensity of 2.2×10^{20} W cm^{-2}, compared with that when HOFs are not included. The enhancement is larger for smaller electron energies and laser beam waists.

It has also been shown that when an electron bunch interacts with a high-intensity tightly-focused fs laser pulse in a co-propagation geometry, attosecond ($\sim$300 as) x-ray pulses can be produced. The photon energy can reach about 40 keV for an electron energy of 2 GeV. The physical scheme investigated in this work can be used for an ultrafast (attosecond or femtosecond) x-ray source in the range of 10–100 keV.

Acknowledgments

This work was supported in part by the BK21 project funded by the Korea Research Foundation and in part by the Basic Research Program (grant no. KRF-2008-313-C00356) funded by Korean Research.

References

[1] Hentschel M *et al* 2001 Attosecond metrology *Nature* **414** 509
[2] Goulielmakis E *et al* 2008 Single-cycle nonlinear optics *Science* **320** 1614
[3] Drescher M *et al* 2002 Time-resolved atomic inner-shell spectroscopy *Nature* **419** 803
[4] Uiberacker M *et al* 2007 Attosecond real-time observation of electron tunnelling in atoms *Nature* **446** 627
[5] Cavalieri A L *et al* 2007 Attosecond spectroscopy in condensed matter *Nature* **449** 1029
[6] Lax M, Louisell W H and McKnight W B 1975 From Maxwell to paraxial wave optics *Phys. Rev.* A **11** 1365
[7] Davis L W Theory of electromagnetic beams *Phys. Rev.* A **19** 1177
[8] Barton J P and Alexander D R 1989 Fifth-order corrected electromagnetic field components for a fundamental Gaussian beam *J. Appl. Phys.* **66** 2800
[9] Scully M O and Zubairy M S 1991 Simple laser accelerator: optics and particle dynamics *Phys. Rev.* A **44** 2656
[10] Salamin Y I 2007 Fields of a Gaussian beam beyond the paraxial approximation *Appl. Phys.* B **86** 319
[11] Salamin Y I and Keitel C H 2002 Electron acceleration by a tightly focused laser beam *Phys. Rev. Lett.* **88** 095005

[12] Huang S, Wu F and Zhao X 2007 Electron acceleration by a focused laser pulse in a static magnetic field *Phys. Plasmas* **14** 123107
[13] Wang P X, Ho Y K and Tang Ch X 2007 Field structure and electron acceleration in a laser beam of a high-order Hermite–Gaussian mode *J. Appl. Phys.* **101** 083113
[14] Lee H, Chung S, Lee K and Kim D 2008 A study of the Thomson scattering of radiation by a relativistic electron of a tightly-focused, co-propagating femtosecond laser beam *New J. Phys.* **10** 093024
[15] Masuda S, Kando M, Kotaki H and Nakajima K 2005 Suppression of electron scattering by the longitudinal components of tightly focused laser fields *Phys. Plasmas* **12** 013102
[16] Lee K, Cha Y H, Shin M S, Kim B H and Kim D 2003 Relativistic nonlinear Thomson scattering as attosecond x-ray source *Phys. Rev.* E **67** 026502
[17] Jackson J D 1999 *Classical Electrodynamics* 3rd edn (New York: Wiley)